

ENTROPY GENERATION MINIMIZATION: THE METHOD AND ITS APPLICATIONS

Adrian Bejan

Department of Mechanical Engineering and Materials Science,
Duke University,
Durham, NC 27708-0300, USA

ABSTRACT

This lecture outlines the basis for the entropy generation minimization method, and a series of key applications in power generation, refrigeration, and energy conservation. The lecture begins with a review of the concept of irreversibility, entropy generation, or exergy destruction. The proportionality between exergy destruction and entropy generation is used in the search for improved thermodynamic performance subject to finite-size constraints and specified environmental conditions. Examples are drawn from refrigeration, energy storage systems for sensible heat and latent heat, solar energy, and the generation of maximum power by using a stream of hot gas. It is shown that the physical structure of the system springs out of the process of global thermodynamic optimization subject to global constraints. This principle generates structure not only in engineering but also in physics and biology (constructal theory).

INTRODUCTION

In this lecture I review some of the changes that have occurred in engineering thermodynamics, and the applications that stand to benefit from these changes. The focus is on the increasingly important role played by thermodynamics (especially the second law) in problem formulation, modeling and design optimization.

The methods of exergy analysis (EA), entropy generation minimization (EGM) and thermoeconomics (TE) are the most established changes that have taken place in modern engineering thermodynamics (Bejan et al., 1996; Moran and Sciubba, 1994; Feidt, 1987; Stecco and Moran, 1990, 1992; Valero and Tsatsaronis, 1992; Boehm, 1997; Faghri and Sunden, 1998; Bejan, 1996a,b; Bejan and Mamut, 1999).

The emphasis is now on identifying the mechanisms and system components that are responsible for thermodynamic losses (EA), the sizes of these losses (EA), minimizing the losses subject to the global constraints of the system (EGM), and minimizing the total costs associated with building and operating the energy system (TE).

The method of thermodynamic optimization or entropy generation minimization (EGM) established itself as a distinct field of activity at the interface between heat transfer, engineering thermodynamics, and fluid mechanics. The position of the field is illustrated in Fig. 1, which is reproduced from the first book published on this method

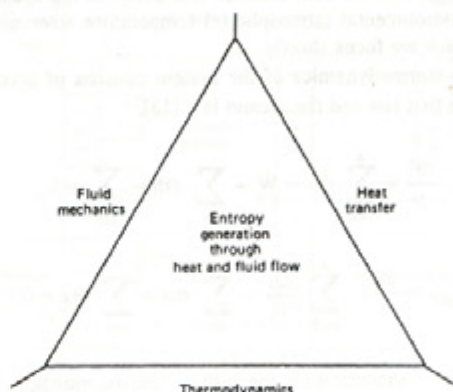


Figure 1: The interdisciplinary field covered by the method of thermodynamic optimization, entropy generation minimization, or finite time thermodynamics (Bejan, 1982).

(Bejan, 1982). The method relies on the simultaneous application of principles of heat and mass transfer, fluid mechanics, and engineering thermodynamics, in the pursuit of realistic models of processes, devices, and installations. By realistic models we mean models that account for the inherent irreversibility of engineering systems.

Thermodynamic optimization may be used by itself (without cost minimization) in the preliminary stages of design, in order to identify trends and the existence of optimization opportunities. The optima and structural characteristics identified based on thermodynamic optimization can be made more realistic through subsequent refinements based on global cost minimization. Thermodynamic optimization may be used especially in areas where the total cost of the installation is dominated by the low temperatures, where the power requirement is substantial cost due to thermodynamic irreversibility. The classical example of this kind is cryogenics, or refrigeration at very and proportional to the entropy generated in the cold space. Many other applications are found in power generation and energy conservation, as shown by the examples collected in this paper.

THERMODYNAMICS COMBINED WITH HEAT TRANSFER AND FLUID MECHANICS

Here is why in thermodynamic optimization we must rely on heat transfer and fluid mechanics, not just thermodynamics. Consider the most general system-environment configuration, namely a system that operates in the unsteady state. Its instantaneous inventories of mass, energy, and entropy are M , E , and S . The system experiences the net work transfer rate \dot{W} , heat transfer rates $(\dot{Q}_0, \dot{Q}_1, \dots, \dot{Q}_n)$ with $n + 1$ temperature reservoirs (T_0, T_1, \dots, T_n) , and mass flow rates $(\dot{m}_{in}, \dot{m}_{out})$ through any number of inlet and outlet ports. Noteworthy in this array of interactions is the heat transfer rate between the system and the environmental (atmospheric) temperature reservoir, \dot{Q}_0 , on which we focus shortly.

The thermodynamics of the system consists of accounting for the first law and the second law [13],

$$\frac{dE}{dt} = \sum_{i=0}^n \dot{Q}_i - \dot{W} + \sum_{in} \dot{m}h - \sum_{out} \dot{m}h \quad (1)$$

$$\dot{S}_{gen} = \frac{dS}{dt} - \sum_{i=0}^n \frac{\dot{Q}_i}{T_i} - \sum_{in} \dot{m}s + \sum_{out} \dot{m}s \geq 0, \quad (2)$$

where h is shorthand for the sum of specific enthalpy, kinetic energy, and potential energy of a particular stream at the boundary. In eq. (2) the total entropy generation rate \dot{S}_{gen} is simply a definition (notation) for the entire quantity on the left-hand side of the inequality sign. We shall see that it is advantageous to decrease \dot{S}_{gen} ; this can be accomplished by

changing at least one of the quantities (properties, interactions) specified along the system boundary.

We select the environmental heat transfer \dot{Q}_0 as the interaction that is allowed to float as \dot{S}_{gen} varies. Historically, this choice was inspired (and justified) by applications to power plants and refrigeration plants, because the rejection of heat to the atmosphere was of little consequence in the overall cost analysis of the design. Eliminating \dot{Q}_0 between eqs. (1) and (2) we obtain

$$\dot{W} = -\frac{d}{dt}(E - T_0S) + \sum_{i=1}^n \left(1 - \frac{T_0}{T_i}\right) \dot{Q}_i + \sum_{in} \dot{m}(h - T_0s) - \sum_{out} \dot{m}(h - T_0s) - T_0\dot{S}_{gen} \quad (3)$$

The power output in the limit of reversible operation ($\dot{S}_{gen} = 0$) is

$$\dot{W}_{rev} = -\frac{d}{dt}(E - T_0S) + \sum_{i=1}^n \left(1 - \frac{T_0}{T_i}\right) \dot{Q}_i + \sum_{in} \dot{m}(h - T_0s) - \sum_{out} \dot{m}(h - T_0s) \quad (4)$$

In engineering thermodynamics each of the terms on the right-hand side of eq. (4) is recognized as an exergy of one type or another [2, 11-13], and the calculation of \dot{W}_{rev} is known as exergy analysis. Subtracting equation (3) from eq. (4) we arrive at the Gouy-Stodola theorem,

$$\dot{W}_{rev} - \dot{W} = T_0\dot{S}_{gen} \quad (5)$$

In eq. (5) \dot{W}_{rev} is fixed because all the heat and mass flows (other than \dot{Q}_0) are fixed.

Pure thermodynamics (e.g., exergy analysis) ends, and EGM begins with eq. (5). The lost power ($\dot{W}_{rev} - \dot{W}$) is always positive, regardless of whether the system is a power producer (e.g., power plant) or a power user (e.g., refrigeration plant). To minimize lost power when \dot{W}_{rev} is fixed is the same as maximizing power output in a power plant, and minimizing power input in a refrigeration plant. This operation is also equivalent to minimizing the total rate of entropy generation. If \dot{W}_{rev} is not held fixed while the system design is being changed, then eq. (5) and the calculation of \dot{S}_{gen} lose their usefulness.

The critically new aspect of the EGM method—the aspect that makes the use of thermodynamics insufficient, and distinguishes EGM from exergy analysis—is the

minimization of the calculated entropy generation rate. To minimize the irreversibility of a proposed design, the analyst must use the relations between temperature differences and heat transfer rates, and between pressure differences and mass flow rates. The analyst must express the thermodynamic nonideality of the design \dot{S}_{gen} as a function of the physical characteristics of the system, namely to finite dimensions, shapes, materials, finite speeds, and finite-time intervals of operation. For this the analyst must rely on heat transfer and fluid mechanics principles, in addition to thermodynamics. Only by varying one or more of the physical characteristics of the system, can the analyst bring the design closer to the operation characterized by minimum entropy generation subject to size and time constraints. We illustrate this technique by means of a few very basic models.

HISTORY: LOW TEMPERATURE REFRIGERATION

To appreciate the engineering origins of the thermodynamic optimization method (EGM), it is useful to recall that the field of low temperature refrigeration was the first where irreversibility minimization became an established method of optimization and design. As a special application of eq. (5), it is easy to prove that the power required to keep a cold space cold is equal to the total rate of entropy generation times the ambient temperature, with the observation that the entropy generation rate includes the contribution made by the leakage of heat from T_0 into the cold space (Bejan, 1982, 1988). The structure of a cryogenic system is in fact dominated by components that leak heat, e.g., mechanical supports, radiation shields, electric cables, and counterflow heat exchangers (Fig. 2). The minimization of entropy generation along a heat leak path consists of optimizing the path in harmony with the rest of the refrigerator or liquefier.

Figure 3 shows a mechanical support of length L that connects the cold end of the machine (T_L) to room temperature (T_H). The rate of entropy generation inside the support shown as a vertical column is

$$\dot{S}_{gen} = \int_{T_L}^{T_H} \frac{\dot{Q}}{T^2} dT \quad (6)$$

where it is important to note that the heat leak \dot{Q} is allowed to vary with the local temperature T . The origin of the integrand in eq. (6) is the infinitesimal element (shaded in Figure 3), in which the rate of entropy generation is $dS_{gen} = \dot{Q}/T + d\dot{Q}/T - (\dot{Q} + d\dot{Q})/(T + dT) = \dot{Q}dT/T^2$. The local heat leak decrement $d\dot{Q}$ is removed by the rest of the installation, which is modeled as reversible. The heat leak is also related to the local temperature gradient and conduction cross-section A ,

$$\dot{Q} = kA \frac{dT}{dx} \quad (7)$$

where the thermal conductivity $k(T)$ decreases toward low temperatures. Rearranged and integrated from end to end, eq. (7) places a size constraint on the unknown function $Q(T)$,

$$\frac{L}{A} = \int_{T_L}^{T_H} \frac{k}{\dot{Q}} dT \quad (8)$$

According to variational calculus, the heat leak function that minimizes the \dot{S}_{gen} integral (6) subject to the finite-size constraint (8) is obtained by finding the extremum of the aggregate integral $\int_{T_L}^{T_H} FdT$ whose integrand F is a linear combination of the integrands of eqs. (6) and (7), $F = \dot{Q}/T^2 + \lambda k/\dot{Q}$ and λ is a Lagrange multiplier. The Euler equation reduces in this case to $\partial F/\partial \dot{Q} = 0$, which yields $\dot{Q}_{opt} = (\lambda k)^{1/2}T$. The Lagrange multiplier is determined by substituting \dot{Q}_{opt} into the constraint (8). The results are

$$\dot{Q}_{opt} = \left(\frac{A}{L} \int_{T_L}^{T_H} \frac{k^{1/2}}{T} dT \right) k^{1/2}T \quad (9)$$

$$\dot{S}_{gen,min} = \frac{A}{L} \left(\int_{T_L}^{T_H} \frac{k^{1/2}}{T} dT \right)^2 \quad (10)$$

Equation (6) was provided by thermodynamics and eq. (7) by heat transfer; together they prescribe the optimal design

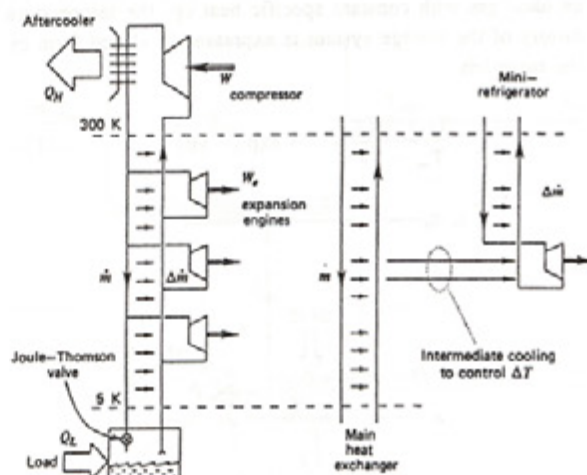


Figure 2: Intermediate cooling of the main counterflow heat exchanger of a helium refrigerator (Bejan, 1982).

(9, 10), which is characterized by a certain distribution of $\dot{Q}(T)$, will generate more entropy and will require more power in order to maintain the cold end of the support at T_L . Quantitative and older examples are given in Bejan (1982, 1996a, 1997). An important example is the main counterflow heat exchanger of any low-temperature refrigeration machine, which must be cooled optimally at intermediate temperatures (e.g., Fig. 2).

Together, eqs. (6) and (8) illustrate the backbone of the method of thermodynamic optimization subject to a physical constraint, as it was practiced in engineering before Bejan and Smith (1974) (this work was reviewed in the first book about the method: Bejan, 1982). In physics, the first application of the method is traced to Curzon and Ahlborn (1975), who rediscovered an optimization problem that had been solved 18 years earlier in engineering by Novikov (1957) and Chambadal (1957). Additional notes on the history of the method in both engineering and physics can be found in Bejan (1996c) and Bejan and Mamut (1999).

SENSIBLE HEAT STORAGE

The opportunity for minimizing the destruction of exergy during energy storage becomes evident if we examine the system shown in Fig. 4. The storage system (the left side of the figure) contains a batch of liquid (m, c). The liquid is held in an insulated vessel. The hot-gas stream \dot{m} enters the system through one port and is gradually cooled as it flows through a heat exchanger immersed in the liquid bath. The spent gas is discharged directly into the atmosphere. As time passes, the bath temperature T and the gas outlet temperature T_{out} approach the hot-gas inlet temperature, T_{in} .

If we model the hot gas (steam, products of combustion) as an ideal gas with constant specific heat c_p , the temperature history of the storage system is expressed in closed form by the equations

$$\frac{T(t) - T_0}{T_{in} - T_0} = 1 - \exp(-y\theta) \quad (11)$$

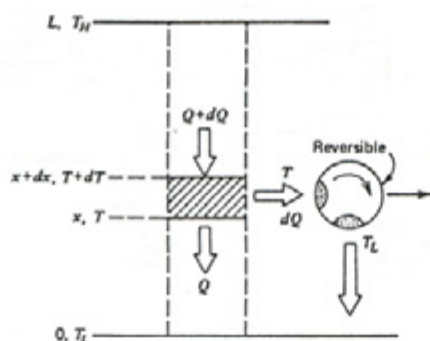


Figure 3: Mechanical support with variable heat leak and intermediate cooling effect (Bejan and Smith, 1974).

$$\frac{T_{out}(t) - T_0}{T_{in} - T_0} = 1 - y \exp(-y\theta) \quad (12)$$

where y and the dimensionless time θ are defined as

$$y = 1 - \exp(-N_{tu}), \quad N_{tu} = \frac{\bar{h}_b A_b}{\dot{m} c_p}, \quad \theta = \frac{\dot{m} c_p}{mc} t \quad (13)$$

In these equations, A_b is the total heat-exchanger surface separating the stream from the liquid bath, and \bar{h}_b is the overall heat transfer coefficient based on A_b . Built into the model is the assumption that the liquid bath is well mixed, i.e., that the liquid temperature (T) is a function of the time (t) only. As expected, both T and T_{out} approach T_{in} asymptotically—the higher the N_{tu} value, the faster.

Turning our attention to the irreversibility of the energy-storage process, Fig. 4 shows that the irreversibility is divided between two distinct parts of the apparatus. First, there is the finite- ΔT irreversibility associated with the heat transfer between the hot stream and the cold liquid bath. Second, the stream exhausted into the atmosphere is eventually cooled down to T_0 , again by heat transfer across a finite ΔT . Neglected in the present model is the irreversibility due to the pressure drop across the heat exchanger traveled by the stream \dot{m} .

The combined effect of the competing irreversibilities noted in Fig. 4 is a characteristic of all sensible-heat storage systems. Because of it, only a fraction of the exergy content of the hot stream can be stored in the liquid bath. In order to see this, consider the instantaneous rate of entropy generation in the overall system delineated in Fig. 4,

$$\dot{S}_{gen} = \dot{m} c_p \ln \frac{T_0}{T_{in}} + \frac{\dot{Q}_0}{T_0} + \frac{d}{dt} (mc \ln T) \quad (14)$$

where $\dot{Q}_0 = \dot{m} c_p (T_{out} - T_0)$. More important than \dot{S}_{gen} is the entropy generated during the entire charging-time

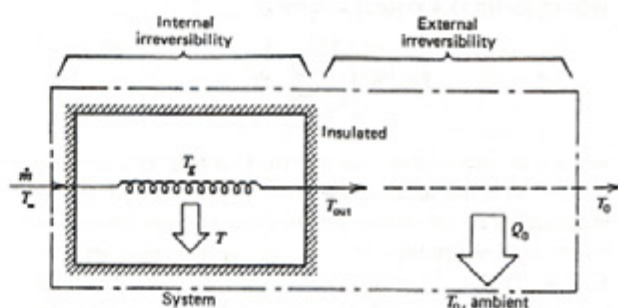


Figure 4: Two sources of irreversibility in the heating phase of a sensible-heat exergy-storage process (Bejan, 1982).

interval $0 - t$, which, using eqs. (11)-(14), can be put in dimensionless form as

$$\frac{1}{mc} \int_0^t \dot{S}_{gen} dt = \theta \left(\ln \frac{T_0}{T_\infty} + \tau \right) + \ln (1 + \tau \eta_I) - \tau \eta_I \quad (15)$$

where the first-law efficiency η_I is shorthand for the right side of eq. (11), and where $\tau = (T_\infty - T_0)/T_0$.

Multiplied by T_0 , the entropy-generation integral $\int_0^t \dot{S}_{gen} dt$ calculated above represents the bite taken by irreversibilities out of the total exergy supply brought into the system by the hot stream:

$$E_x = t \dot{E}_x = t mc_p \ln [T_\infty - T_0 - T_0 \ln (T_\infty / T_0)] \quad (16)$$

On this basis, we define the entropy-generation number N_S as the ratio of the lost exergy divided by the total exergy invested during the time interval $0 - t$:

$$N_S(\theta, \tau, N_{tu}) = \frac{T_0}{E_x} \int_0^t \dot{S}_{gen} dt = 1 - \frac{\tau \eta_I - \ln (1 + \tau \eta_I)}{\theta [\tau - \ln (1 + \tau)]} \quad (17)$$

This entropy-generation number takes values in the range 0-1, the $N_S = 0$ limit representing the elusive case of reversible operation. Note the relation $N_S = 1 - \eta_{II}$, where η_{II} is the second-law efficiency of the installation during the charging process.

Charts of the $N_S(\theta, \tau, N_{tu})$ surface (Bejan, 1982) show that N_S decreases steadily as the heat-exchanger size (N_{tu}) increases. This effect is expected. Less expected is the fact that N_S goes through a minimum as the dimensionless time θ increases. For example, the optimal time for minimum N_S can be calculated analytically in the limit $\tau \ll 1$, where eq. (17) becomes

$$N_S = 1 - [1 - \exp(-\gamma\theta)]^2 / \theta \quad (18)$$

The solution of the equation $\partial N_S / \partial \theta = 0$ is

$$\theta_{opt} = 1.256 [1 - \exp(-N_{tu})]^{-1} \quad (19)$$

In other words, for the common range of N_{tu} values (1-10), the optimal dimensionless charging time is consistently a number of order 1. This conclusion continues to hold as τ takes values greater than 1.

Away from the optimal charging time (i.e., when $\theta \rightarrow 0$ or $\theta \rightarrow \infty$), the entropy-generation number N_S approaches unity. In the short-time limit ($\theta \ll \theta_{opt}$), the entire exergy content

of the hot stream is destroyed by heat transfer to the liquid bath, which was initially at atmospheric temperature T_0 . In the long-time limit ($\theta \gg \theta_{opt}$), the external irreversibility takes over. In this limit, the used stream exits the heat exchanger as hot as it enters ($T_{out} = T_\infty$) and its exergy content is destroyed entirely by the heat transfer (or mixing) with the T_0 atmosphere. The traditional (first-law) rule of thumb of increasing the time of communication between heat source and storage material is counterproductive from the point of view of avoiding the destruction of exergy.

LATENT HEAT STORAGE

A simple way to perform the thermodynamic optimization of the latent heat storage process was proposed by Lim et al. (1992), Fig. 5. The hot stream of initial temperature T_∞ comes in contact with a single phase-change material through a finite thermal conductance UA , assumed known, where A is the heat transfer area between the melting material and the stream, and U is the overall heat transfer coefficient based on A . The phase-change material (solid or liquid) is at the melting point T_m . The stream is well mixed at the temperature T_{out} , which is also the temperature of the stream exhausted into the atmosphere (T_0).

The "steady" operation of the installation of Fig. 5 accounts for the cyclic operation in which every infinitesimally short storage (melting) stroke is followed by a short energy retrieval \dot{m} is stopped, and the recently melted phase-change material is solidified to its original state by the cooling effect provided by the heat engine positioned between T_m and T_0 . In this way, the steady-state model of Fig. 5 represents the complete cycle—that is, storage followed by retrieval.

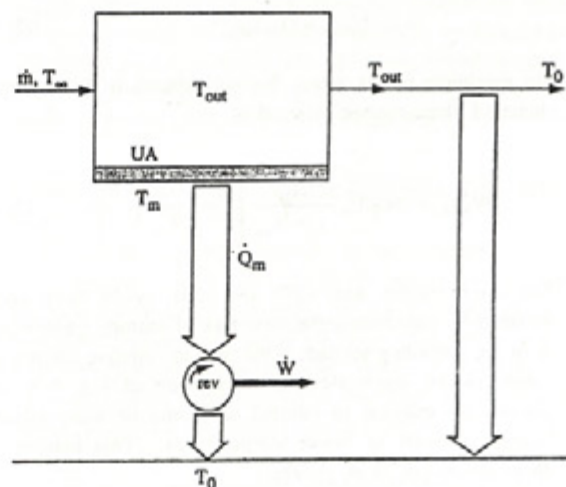


Figure 5: The steady production of power using a single phase-change material and a mixed stream (Lim et al., 1992).

The steady cooling effect of the power plant can be expressed in two ways:

$$\dot{Q}_m = UA(T_{out} - T_m) \quad \dot{Q}_m = \dot{m}c_p(T_{\infty} - T_{out}) \quad (20)$$

By eliminating T_{out} between these two equations we obtain

$$\dot{Q}_m = \dot{m}c_p \frac{N_{tu}}{1 + N_{tu}} (T_{\infty} - T_m) \quad (21)$$

in which N_{tu} is the number of heat transfer units of the heat exchanger surface,

$$N_{tu} = \frac{UA}{\dot{m}c_p} \quad (22)$$

Of interest is the maximum rate of exergy, or useful work (\dot{W} in Fig. 5) that can be extracted from the phase-change material. For this, we model as reversible the cycle executed by the working fluid between T_m and T_0

$$\dot{W} = \dot{Q}_m \left(1 - \frac{T_0}{T_m} \right) \quad (23)$$

and, after combining with eq. (21), we obtain

$$\dot{W} = \dot{m}c_p \frac{N_{tu}}{1 + N_{tu}} (T_{\infty} - T_m) \left(1 - \frac{T_0}{T_m} \right) \quad (24)$$

By maximizing \dot{W} with respect to T_m —that is, with respect to the type of phase-change material, we obtain the optimal melting and solidification temperature:

$$T_{m,opt} = (T_{\infty} T_0)^{1/2} \quad (25)$$

The maximum power output that corresponds to this optimal choice of phase-change material is

$$\dot{W}_{max} = \dot{m}c_p T_{\infty} \frac{N_{tu}}{1 + N_{tu}} \left[1 - \left(\frac{T_0}{T_{\infty}} \right)^{1/2} \right]^2 \quad (26)$$

The same results, eqs. (25) and (26), could have been obtained by minimizing the total rate of entropy generation, as in the preceding section. One way to improve the power output of the single-element installation of Fig. 5 is by placing the exhaust in contact with one or more phase-change elements of lower temperatures. This method is illustrated in Lim et al. (1992).

SOLAR COLLECTORS

The optimization of solar energy conversion has been studied under the banners of two fundamental problems. One

is concerned with establishing the theoretical limits of converting thermal radiation into work, or calculating the exergy content of radiation. The other problem deals with the delivery of maximum power from a solar collector of fixed size (Bejan et al., 1981). This problem has also been solved in many subsequent applications (Bejan 1996a, 1997a), which are united by an important design feature: the collector operating temperature can be optimized.

This optimization opportunity is illustrated in Fig. 6. A power plant is driven by a solar collector with convective heat leak to the ambient. The heat leak is assumed to be proportional to the collector-ambient temperature difference, $\dot{Q}_0 = (UA)_c(T_c - T_0)$. The internal heat exchanger between the collector and the hot end of the power cycle (the user) is modeled similarly, $\dot{Q}_0 = (UA)_i(T_c - T_u)$. There is an optimal coupling between the collector and the power cycle such that the power output is maximum. This design is presented by the optimal collector temperature (Bejan, 1982)

$$\frac{T_{c,opt}}{T_0} = \frac{\theta_{max}^{1/2} + R\theta_{max}}{1 + R} \quad (27)$$

where $R = (UA)_c/(UA)_i$ and $\theta_{max} = T_{c,max}/T_0$ is the maximum (stagnation) temperature of the collector. This optimum has its origin in the trade-off between the Carnot efficiency of the reversible part of the power plant ($1 - T_0/T_u$) and the heat loss to the ambient, \dot{Q}_0 . The power output is the product $\dot{Q}(1 - T_0/T_u)$. When $T_c < T_{c,opt}$ the Carnot factor is too small. When $T_c > T_{c,opt}$ the heat input \dot{Q} drawn from the collector is too small, because the heat loss to the ambient \dot{Q}_0 is large.

Corresponding optimal couplings have been identified in solar-driven power plants of many power-cycle designs, extraterrestrial power plants, and refrigeration systems driven by solar power (Bejan 1996a, 1997a).

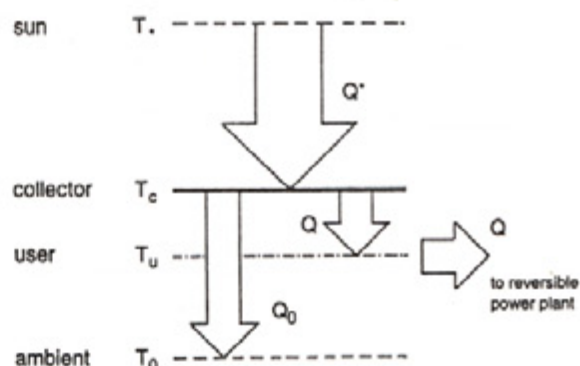


Figure 6: Solar power plant model with collector-ambient heat loss and collector-power cycle heat exchanger (Bejan et al., 1981).

DISTRIBUTION OF HEAT TRANSFER AREA

Heat transfer principles combined with thermodynamics shed light on why energy systems are imperfect, and why they possess geometric structure—why their hardware is arranged in certain amounts, and in certain ways in space. A power plant owes its irreversibility to many factors, one of which is the transfer of heat across finite temperature differences. This effect has been isolated in Fig. 7. The power plant is the vertical segment marked between the high temperature T_H and the ambient temperature T_L . The heat input Q_H (fixed) and the rejected heat Q_L must be driven by temperature differences: the temperature gaps $T_H - T_{HC}$ and $T_{LC} - T_L$ account for some of the space occupied by the power plant. Heat transfer surfaces reside in these spaces. The rest of the space is reserved for the rest of the power plant: for simplicity, this inner space is assumed to be irreversibility free.

$$S_{gen} = \frac{Q_L}{T_{LC}} - \frac{Q_H}{T_{HC}} = 0 \quad (28)$$

All the irreversibility of this power plant model is concentrated in the two temperature gaps. The simplest heat transfer model for these is the proportionality between heat current and temperature difference.

$$Q_H = C_H(T_H - T_{HC}) \quad Q_L = C_L(T_{LC} - T_L) \quad (29, 30)$$

Each thermal conductance (C_H, C_L) is proportional to its area for heat transfer. This is why the simplest way to account for the finiteness of the heat transfer surface available to the power plant is to recognize the constraint (Bejan, 1988)

$$C_H + C_L = C \quad (31)$$

where C is fixed. This constraint is adequate when the overall heat transfer coefficients of the two surfaces are equal. More general constraints, valid for unequal heat transfer coefficients, can also be used.

The analytical model is completed by the first law, written for the power plant as a closed system operating in steady state or in an integral number of cycles, $W = Q_H - Q_L$. Combining this with the preceding relations, we obtain the power output as a function of the conductance allocation fraction $x = C_H/C$,

$$\frac{W}{Q_H} = 1 - \frac{T_L/T_H}{1 - \frac{Q_H}{T_{HC}} \left(\frac{1}{x} + \frac{1}{1-x} \right)} \quad (32)$$

This expression can be maximized with respect to x , and the result is $x_{opt} = 1/2$, or

$$C_{H,opt} = C_{L,opt} \quad (33)$$

In conclusion, there is an optimal way to allocate the constrained hardware (C) to the two ends of the power plant, that is, if the maximization of power output subject to fixed heat input (Q_H) and fixed size (C) is the purpose. Equation (33) also holds for refrigerating machines modeled in the same way.

The maximization of W is shown graphically in Fig. 7. Small conductances strangle the flow of heat, and demand large temperature differences. The power output is large when the temperature difference across the reversible compartment is large. The first and third frames of Fig. 7 show that when the two conductances are highly dissimilar in size, large temperature gaps are present, and the power output is small. The best irreversible performance is somewhere in the middle, where the conductances are comparable in size.

EXERGY EXTRACTION FROM A STREAM OF HOT GAS

Thermodynamics alone provides an unambiguous answer to the question of the maximum power that is theoretically available from a stream solely in the presence of the atmospheric temperature reservoir (T_0): that answer is the 'flow exergy' of the stream (Moran, 1989). It is helpful to review this result while looking at the upper part of Fig. 8 and assuming that the stream is single-phase, for example, an ideal gas. If the hot stream (\dot{m}, T_H) makes contact with a reversible device while reaching thermal equilibrium with the ambient before it is discharged, and if the pressure drop along the stream is assumed negligible, the power output is

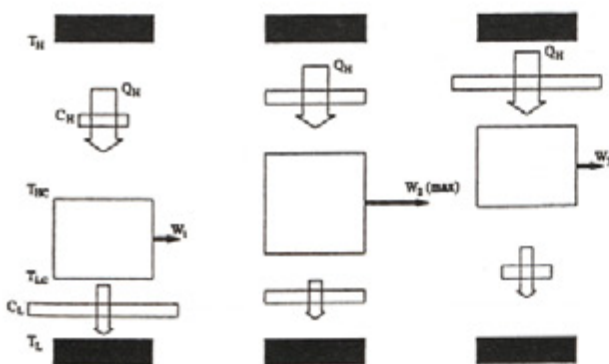


Figure 7: Model of power plant with two heat transfer surfaces, and the maximization of power output subject to fixed heat input (Q_H) and fixed total heat transfer surface (C).

$$\dot{W}_{rev} = \dot{m}c_p T_0 \left(\frac{T_H}{T_0} - 1 - \ln \frac{T_H}{T_0} \right) \quad (34)$$

The actual power output will always be lower than \dot{W}_{rev} because of the irreversibility of the heat transfer between the hot stream and the rest of the power plant. A first step in the direction of accounting for the heat transfer irreversibility is the model of Fig. 8, where the heat transfer surface has the finite size $A = pL$, and p is the heat transfer area per unit of flow path length. The power producing compartment is a succession of many reversible compartments of the kind shown in the center of the figure. The infinitesimal power output is

$$d\dot{W} = \left[1 - \frac{T_0}{T_s(x)} \right] d\dot{Q}_H \quad (35)$$

where the temperature is plotted on the vertical in Fig. 8, and $d\dot{Q}_H = \dot{m}c_p dT$. The heat transfer through the surface A is assumed proportional to the local temperature difference,

$$d\dot{Q}_H = [T(x) - T_s(x)] U p dx \quad (36)$$

where U is the overall heat transfer coefficient, which is assumed constant. Combining these equations and integrating from $x = 0$ to $x = L$ ($= A/p$) we arrive at the total power output and the finite-area constraint:

$$\dot{W} = \int_{T_{out}}^{T_H} \left(1 - \frac{T_0}{T_s} \right) \dot{m}c_p dT \quad (37)$$

$$\int_{T_{out}}^{T_H} \frac{dT}{T - T_s} = \frac{UA}{\dot{m}c_p} = N_{tu} \quad (38)$$

An alternate route to calculating the power output \dot{W} is to apply the Gouy-Stodola theorem (5) to the larger system (extended with dashed line) in Fig. 8. The reversible-limit power output \dot{W}_{rev} corresponds to the reversible cooling of the stream from T_H all the way down to T_0 . The entropy

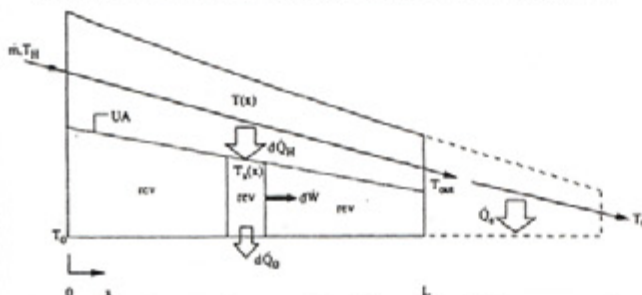


Figure 8: Power plant model with unmixed hot stream in contact with a nonisothermal heat transfer surface (Bejan and Errera, 1998).

generation rate \dot{S}_{gen} is the total amount associated with the larger system, and is due to two sources: the temperature difference $T - T_s$, and the finite temperature difference required by the external cooling rate $\dot{Q}_c = \dot{m}c_p(T_{out} - T_0)$. These two contributions are represented by the two terms in the expression

$$\dot{S}_{gen} = \int_{T_{out}}^{T_H} \left(\frac{1}{T_s} - \frac{1}{T} \right) \dot{m}c_p dT + \left(\dot{m}c_p \ln \frac{T_0}{T_{out}} + \frac{\dot{Q}_c}{T_0} \right) \quad (39)$$

To maximize \dot{W} is equivalent to minimizing \dot{S}_{gen} , because \dot{W}_{rev} is fixed. The entropy generation rate (39) is subject to the size constraint (38). There are two degrees of freedom in the minimization of \dot{S}_{gen} : the shape of the surface temperature function $T_s(x)$, and the place of this function on the temperature scale (i.e., closer to T_H or T_0). The second degree of freedom is alternately represented by the value of the exhaust temperature T_{out} . The optimization of the function $T_s(x)$ is accomplished based on variational calculus (Bejan and Errera, 1998):

$$T_{s,opt}(x) = \mu T_H \exp \left(- \frac{x}{L} \ln \frac{T_H}{T_{out}} \right) \quad (40)$$

$$\mu = 1 - \frac{1}{N_{tu}} \ln \frac{T_H}{T_{out}} \quad (41)$$

$$T_{opt}(x) = T_H \exp \left(- \frac{x}{L} \ln \frac{T_H}{T_{out}} \right) = \frac{1}{\mu} T_{s,opt} \quad (42)$$

$$\dot{W}_{max} = \dot{m}c_p T_0 \left(\frac{T_H}{T_0} - \frac{T_{out}}{T_0} - \frac{1}{\mu} \ln \frac{T_H}{T_{out}} \right) \quad (43)$$

At any x , the temperature difference $(T - T_s)$ is proportional to the local absolute temperature. This optimal distribution of temperatures is illustrated in Fig. 9.

The second step of the minimization of exergy destruction consists of maximizing numerically the expression (43) with respect to T_{out} . The result is the twice-maximized power output $\dot{W}_{max,max}$ reported in dimensionless form in Fig. 10,

$$\dot{W}_{mm} = \dot{W}_{max,max} / (\dot{m}c_p T_0) \quad (44)$$

It can be verified that this rate of exergy production approaches the reversible limit (34) as the surface size (N_{tu}) increases.

The deduced proportionality between $(T - T_s)$ and T (or T_s) means that this optimal configuration can be implemented in practice by using a single-phase stream $(\dot{m}c_p)_s$ in place of the $T_s(x)$ surface: this stream runs in counterflow relative to

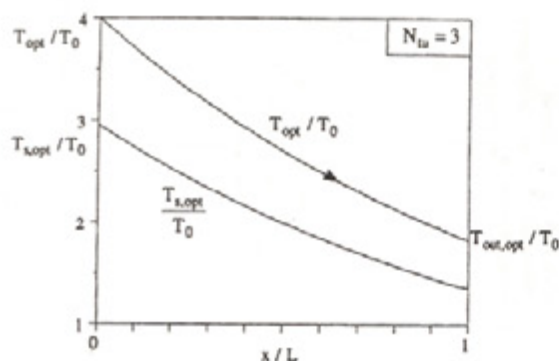


Figure 9: The optimal distribution of temperature along the stream and the heat transfer surface of Figure 8 (Bejan and Errera, 1998).

the hot stream m . The counterflow is characterized by a certain, optimal imbalance (the ratio between the capacity flow rates of the two streams), which is the result of thermodynamic optimization, and is reported in Fig. 11.

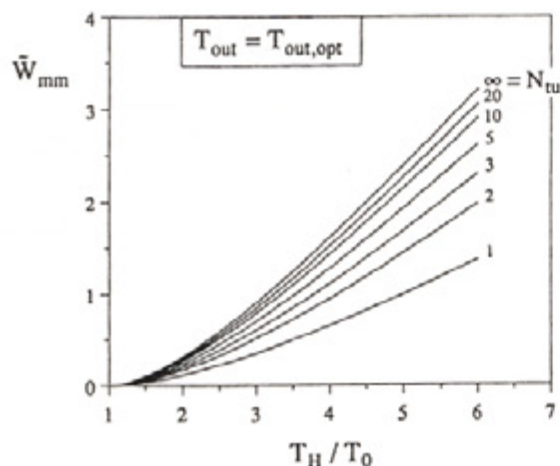


Figure 10: The twice maximized power output corresponding to the model of Figure 8 (Bejan and Errera, 1998).

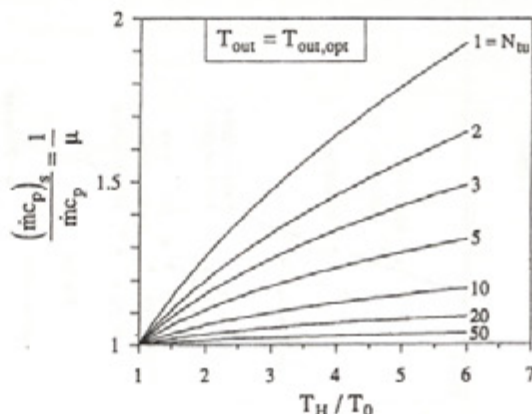


Figure 11: The optimal imbalance of the counterflow heat exchanger used in conjunction with the model of Figure 8 (Bejan and Errera, 1998).

GEOMETRY SPRINGS OUT OF THERMODYNAMIC OPTIMIZATION

In the preceding section, the maximization of exergy extraction (\dot{W}) subject to fixed size (A) led to the physical structure of the flow system: the counterflow heat exchanger, and its optimal imbalance. The alternative is to minimize A subject to specified (\dot{W}), and in this case the optimal structure turns out to be the same. In all the examples reviewed in this paper, the physical result of global optimization of thermodynamic performance was *structure*. This structure-generating principle deserves to be pursued further, in increasingly more complex system configurations. The generation of structure in engineering has been named *constructal method*; the thought that the same principle accounts for the generation of shape and structure in natural flow systems is *constructal theory* (Bejan, 2000).

The principle of organizing structure for the purpose of extracting and using maximum exergy from a hot stream is particularly relevant to the integrative conceptual design of energy flow systems for aircraft. The same principle applies to systems in which all the functions are driven by the exergy drawn from the limited fuel installed on board: ships, automobiles, military vehicles, environmental-control suits, portable power tools, etc. Additional support for this view is provided by the record on powered flight, engineered and natural. Figure 12 shows the cruising speeds of insects, birds and airplanes, next to the theoretical speed obtained by minimizing the power (exergy rate) destroyed during flight (Bejan, 2000).

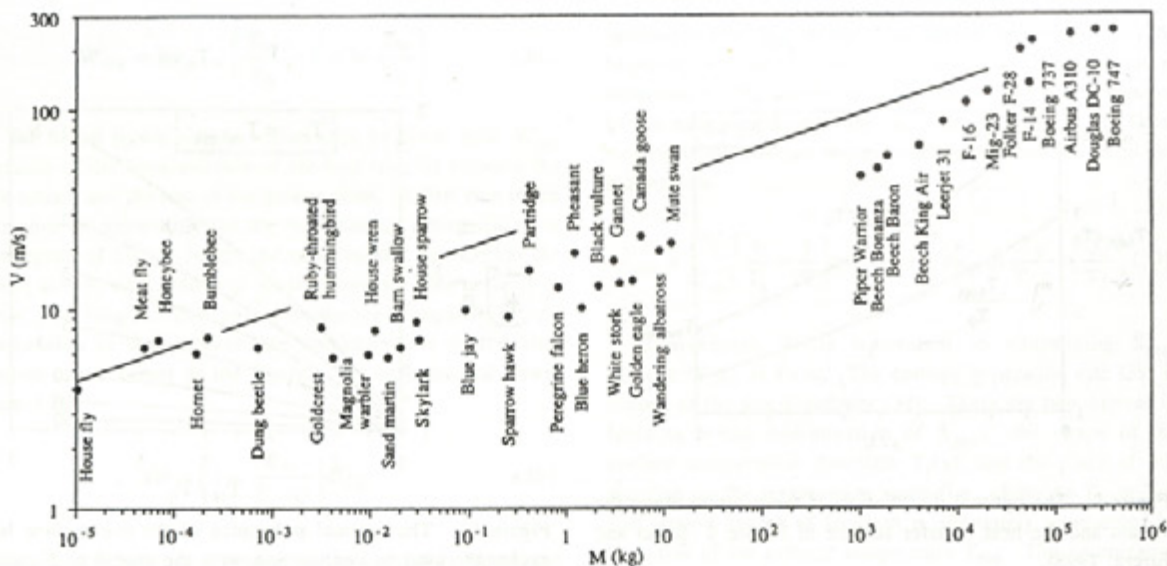


Figure 12: Cruising speeds of insects, birds and airplanes, and the theoretical speed for minimum rate of exergy destruction during flight (the solid line) (Bejan, 2000).

The performance record of the natural and engineered flow systems (e.g., Fig. 12) suggests that the constructal principle is important not only in engineering but also in physics and biology in general. In this theoretical framework the airplane emerges as a physical extension of man, in the same way that the body of the flying animal (e.g., bat, bird) developed its own well adapted extensions. All such extensions are evolutionary, discrete marks on a continuous time axis that points toward the better and the more complex. This theoretical line of inquiry is explored in a new book (Bejan, 2000).

REFERENCES

- Bejan, A., 1982, *Entropy Generation through Heat and Fluid Flow*, Wiley, New York.
- Bejan, A., 1988, *Advanced Engineering Thermodynamics*, Wiley, New York.
- Bejan, A., 1996a, *Entropy Generation Minimization*, CRC Press, Boca Raton, FL.
- Bejan, A., 1996b, Entropy generation minimization: the new thermodynamics of finite-size devices and finite-time processes, *J. Appl. Phys.*, vol. 79, pp. 1191-1218.
- Bejan, A., 1996c, Notes on the history of the method of entropy generation minimization (finite time thermodynamics), *J. Non-Equilib. Thermodyn.*, vol. 21, pp. 239-242.
- Bejan, A., 1997a, *Advanced Engineering Thermodynamics*, second edition, Wiley, New York.
- Bejan, A., 2000, *Shape and Structure, from Engineering to Nature*, Cambridge University Press, Cambridge, UK.
- Bejan, A. and Errera, M. R., 1998, Maximum power from a hot stream, *Int. J. Heat Mass Transfer*, vol. 41, pp. 2025-2036.
- Bejan, A. and Mamut, E., eds., 1999, *Thermodynamic Optimization of Complex Energy Systems*, Kluwer Academic Publishers, Dordrecht, The Netherlands.
- Bejan, A. and Smith, Jr., J. L., 1974, Thermodynamic optimization of mechanical supports for cryogenic apparatus, *Cryogenics*, vol. 14, pp. 158-163.
- Bejan, A. Kearney, D. W. and Kreith, F., 1981, Second law analysis and synthesis of solar collector systems, *J. Solar Energy Eng.*, vol. 103, pp. 23-30.
- Bejan, A., Tsatsaronis, G. and Moran, M., 1996, *Thermal Design and Optimization*, Wiley, New York.
- Boehm, R. F., ed., 1997, *Developments in the Design of Thermal Systems*, Cambridge University Press, Cambridge, UK.
- Chambadal, P., 1957, *Les Centrales Nucleaires*, Armand Colin, Paris.
- Curzon, F. L. and Ahlborn, B., 1975, Efficiency of a Carnot Engine at Maximum Power Output, *Am. J. Phys.*, vol. 43, pp. 22-24.
- Faghri, M. and Sunden, B., eds. 1998, *Modeling of Engineering Heat Transfer Phenomena*, Computational Mechanics Publications, Southampton, UK.
- Feidt, M., 1987, *Thermodynamique et Optimisation Énergetique des Systèmes et Procédés*, Technique et Documentation, Lavoisier, Paris.
- Lim, J. S., Bejan, A. and Kim, J. H., 1992, Thermodynamic optimization of phase-change energy storage using two or more materials, *J. Energy Resources Technology*, vol. 114, pp. 84-90.
- Moran, M. J., 1989, *Availability Analysis: A Guide to*

- Efficient Energy Use*, ASME Press, New York.
- Moran, M. J. and Sciubba, E., 1994, Exergetic analysis: principles and practice, *J. Eng. Gas Turbines Power*, vol. 116, pp. 285-290.
- Novikov, I. I., 1957, The efficiency of atomic power stations, *At. Energ.*, vol. 3, p. 409; English translation in 1958, *J. Nuclear Energy II*, vol. 7, pp. 125-128.
- Stecco, S. S. and Moran, M. J., eds., 1990, *A Future for Energy*, Pergamon, Oxford, UK.
- Stecco, S. S. and Moran, M. J., eds., 1992, *Energy for the Transition Age*, Nova Science, New York.
- Valero, A. and Tsatsaronis, G., eds., 1992, *ECOS '92, Proc. Int. Symp. Efficiency, Costs, Optimization and Simulation of Energy Systems*, Zaragoza, Spain, ASME Press, New York.